Int. J. Nano Dimens., 12 (3): 211-221, Summer 2021

ORIGINAL ARTICLE

Eco-friendly synthesis of surface grafted Carbon nanotubes from sugarcane cubes for the development of prolonged release drug delivery platform

Rahul Narkhede[1], Mahesh More[2], Swapnil Patil[1], Pravin Patil[3], Ashwini Patil[4], Prashant Deshmukh[5*]

[1] Post Graduate Department of Pharmaceutics, H. R. Patel Institute of Pharmaceutical Education and Research, Shirpur, Dhule -425405 (M. S.), India
[2] Department of Pharmaceutics, Sanjivani College of Pharmaceutical Education and Research, Kopargaon, Dist – Ahemadnagar - 423 603 (M.S.) India
[3] Department of Pharmaceutical Chemistry, H. R. Patel Institute of Pharmaceutical Education and Research, Shirpur, Dhule -425405 (M. S.), India
[4] Department of Microbiology and Biotechnology, R.C.Patel Arts, Science, and Commerce College, Shirpur, Dhule -425405 (M. S.) India
[5] Department of Pharmaceutics, Dr. Rajendra Gode College of Pharmacy, Malkapur, Dist – Buldhana – 443 101 (M.S.), India

Received 12 January 2021; revised 27 February 2021; accepted 05 April 2021; available online 15 April 2021

Abstract

Surface grafting of nanocarriers could modulate their properties and characteristics. As carbon nanotubes synthesis is a very tricky process and requires high-end methods, hence the present investigation was aimed to develop an eco-friendly method for synthesis carbon nanotubes (CNTs) and subsequent surface grafting for enhanced drug delivery application. The present study elaborates two-step chemical modifications; wherein the first step is catalytic cleavage of natural precursor in the presence of ferrocene and the second step involve chemical grafting of Acyclovir (ACV) as a model drug to understand the drug release behaviour. The catalytic cleavage of sugarcane cubes (natural precursor) was carried out in a closed copper tube, which prevents oxidation and results in a conversion of tubular nanostructures to amorphous carbon. The covalent attachment of ACV on purified CNTs (fCNTs) was done using carbodiimide chemistry. The preliminary Uv-Vis absorbance spectra defined at 260 nm was arised due to π-π* stacking of aromatic C-C bonds. The Fourier Transforms Infrared Spectroscopy (FTIR) indicates the hydroxyl stretch at 3300 cm-1 while amide I bond formation was observed at 1672 cm^{-1}. The XRD spectra confirmed successful synthesis of CNTs. The calculated average crystallite size (Scherer equation) of synthesized CNTs was found to be 42.84 and 44.45 nm; it was also in accordance with the morphological observation as confirmed simultaneously using SEM analysis. The covalently attached ACV was released up to 80% during 8h of *in vitro* drug release study. The surface grafting potential of CNTs was found to be promising compared to other nanomaterials.

Keywords: *Acyclovir; Amorphous Carbon; Carbodiimide Chemistry; Natural Precursor; Purification.*

How to cite this article

Narkhede R., More M., Patil S., Patil P., Patil A., Deshmukh P. Eco-friendly synthesis of surface grafted Carbon nanotubes from sugarcane cubes for the development of prolonged release drug delivery platform. Int. J. Nano Dimens., 2021; 12(3): 211-221.

INTRODUCTION

Even though the investigation on allotropic forms of carbon was begun before 1990, but the most intuitive form of carbon allotrope i.e. carbon nanotubes (CNTs) were reported in 1991[1]. Numerous classical approaches for the synthesis of CNTs are reported by academic researchers and industry experts for their promising physicochemical properties. In case of CNTs, the

* Corresponding Author Email: *pkdesh@rediffmail.com*

two-dimensional (2D) structure may be elongated in several meter length with nanometre size in diameter. This 2D structure of CNTs could also be constructed from the graphite sheet by rolling down to cylindrical counterparts [2]. The CNTs are structurally distinct from graphene sheets and could be of several layers one around the other, resulting in different classes such as Single-walled CNTs (SWCNTs), Double-walled CNTs (DWCNTs), Multi-walled CNTs (MWCNTs), to name a few [3].

There are plenty of methods available for the synthesis of CNTs, but all these procedures involve harsh reaction conditions which generates unavoidable toxic gases. These gases may produce deleterious effects on the environment. Many of these techniques are highly sophisticated and expensive as well [4]. Several researchers have reported use of ferrocene as a promising catalyst for the synthesis of CNTs. Ferrocene starts nucleating in high-temperature environments and activates iron clusters for the initiation and growth of nanotubes. The transition metal particles starts the growth of CNTs from centre proximity during the synthesis of CNTs from natural precursors [5]. Similarly, other researchers also explored the bio-precursor derived CNTs in the recent literature [6, 7].

The CNTs are entrenched with incredible mechanical strength, electrical and structural behaviour along with high thermal conductivity [8, 9]. The polyaromatic molecules could easily be absorbed on the electron-rich surfaces of graphitic carbon by hydrogen bonding interaction or Π-Π* interaction. The variety of molecules (proteins, enzyme, drugs, antibodies, DNA, etc.) have an aromatic ring-like arrangement that could be easily conjugated with graphitic carbons [10-12]. Purification is one of the necessary steps after the synthesis of CNTs; purity contributes only about 30–70% of graphitic carbon with the other impurities like amorphous carbon, precursor, catalyst, etc. Chemical oxidation or partial condensation is the most preferred method used by various researchers which consists of one or more oxidizing agents. The purification process can help to enhance the water dispersibility of CNTs as oxygen-containing groups are grafted on the surfaces [13-15].

The tuneable surface properties and longer tube length of CNTs can improve the loading efficiency and transportation across the cells [16]. The CNTs also protects the therapeutic molecules from endogenous enzymatic degradation. Hence, it can be referred as a 'smart vehicle' for the drug delivery directly inside the cell due to its ability as a penetrating agent [17].

In the present investigation, we have demonstrated the simple and economical process for synthesis and purification of CNTs from a natural source. In this process, the sugar cane cubes (SCB) were used as a natural precursor and ferrocene was employed as a catalyst during optimization. The comparative characterization of CNT and fCNT revealed a significant difference between synthesized and purified CNTs. The carbodiimide chemistry was used to activate surface carboxyl groups of CNTs for active participation in crosslinking reactions. The ACV could form an amide bond with carboxylic moiety of fCNT due to the presence of amine group. The fCNTs demonstrated very prominent delivery properties, loading efficiency, and drug release characteristics.

EXPERIMENTAL

Materials

Sugar cane cubes (SCB) were collected from the local market. Ferrocene was received as a gift sample from Dr. Arunabha Thakur, Asst. Professor (DST), National Institute of Technology, Rourkela, India. Acyclovir (ACV) was kindly gifted by Agog Pharma Ltd., Thane, India. All other chemicals and reagents used were of analytical grade and used as received.

Methodology

Synthesis of carbon nanotubes (CNTs)

The sugarcane was cleaned, peeled off, and cut into small cubes. These cubes were taken into silica crucible and heated in a muffle furnace at 500 ^{0}C for 15 min. The black carbonaceous material obtained after heating was removed and washed multiple times with water and ethanol. It was then mixed with ferrocene in the weight ratios of 10 : 1 by trituration method. The mixture was filled into a closed-loop copper tube and placed into a muffle furnace for 15 min. The furnace was then heated at the rate of 10 ^{0}C/min, to reach the optimum temperature of 500 ^{0}C. The dark black colour carbonaceous material thus obtained was collected, washed with water: ethanol (50:50) mixture. The key optimization was done by varying the temperature and exposure time in the muffle furnace; differential variables were explored and

are provided in Table S1 as a supplementary data.

Purification and functionalization of synthesized CNTs (fCNTs)

The purification and simultaneous functionalization help to remove acid soluble impurities and inorganic content from the reaction mixture. The Piranha solution is most effective in managing the purity of allotropic forms of carbon and grafting carboxyl functionality on the surfaces. The modification helps to increase the water dispersibility of CNTs, which is one of the necessary properties in biomedical applications. Purification was done using the oxidation of the reaction mixture in the presence of nitric acid. The acidic environment helps to dissolve the amorphous carbon, inorganic impurities and promotes oxidation. The synthesized CNTs were ultrasonicated in nitric acid to make homogenous dispersion. The solution was heated at 80 ^{0}C under the reflux with the subsequent addition of 7M ammonium hydroxide (25mL). After a few minutes of reaction, hydrogen peroxide (25 mL) was added in a drop wise manner and the reaction was continued for 6 h. The sample was then centrifuged at 20000 rpm for 30 min and washed with water till neutralization. The remaining dissolved matter was removed by repeated washing with acetone and ethanol; and dried at 40 ^{0}C.

Acyclovir loading on functionalized CNTs (ACV Loaded fCNT – DLCNT)

The fCNT sample was further used to load ACV. The procedure in a brief involves, dispersion of fCNTs (800 mg) in water with subsequent ultra-sonication for 1 h, and the addition of an equivalent amount of ACV in the above solution. The sample was stirred at room temperature at 300 rpm with the subsequent addition of N-(3-Dimethylaminopropyl)-N'-ethyl carbodiimide hydrochloride (EDAC) and N-Hydroxysuccinamide (NHS) as a cross linker to promote the reaction between fCNTs and ACV. The sample was then centrifuged at 12000 rpm for 20 min and washed with water.

CHARACTERIZATION

UV spectrophotometric analysis was performed using UV-Visible Spectrophotometer (UV 1800, Shimadzu, Japan) for the preliminary characterization of synthesized CNT, fCNT, ACV, and DLCNT. The increase in peak intensity indicates the efficiency of the purification process by spectrophotometric observation. UV-Vis spectrophotometric examination was also used to confirm the *in-vitro* drug release pattern, drug content, and encapsulation efficiency from DLCNT using a standard calibration curve of ACV. Similarly, FTIR (Shimadzu 8400S, Japan) was used to confirm synthesized and purified CNTs by analysing prominent functional groups observed in the spectrum. A diffuse reluctant substance (DRS) technique was used for sample analysis. The FTIR spectra of ACV confirmed its authenticity. The analysis spectrum was used to quantify the amide bonding formed between ACV and fCNT.

The particle size and zeta potential analysis was done using NanoPlus 3 particle size analyser (Particulate System, Micrometrics, USA). Identification of synthesized CNT and fCNTs and their crystalline nature was done using X-Ray Diffraction (XRD) analysis which is carried out on D-8, Advance X-ray diffractometer with Cu Kα radiation (k = 0.15418 nm, Bruker, Germany). The Raman analysis of synthesized CNT and fCNT was performed using RENISHAW, Invia Raman spectrometer with a 514 nm laser at a power of 4.7mW. The surface morphology of synthesized CNT and fCNT was analysed using scanning electron microscopy (Bruker, 1530-2 FESEM/ EDX) with an acceleration voltage of 20 kV at 1 µm resolution. The cumulative percentage drug release study was performed using a dialysis bag method [10], wherein samples were withdrawn at a fixed time interval and measured at 256 nm.

RESULT AND DISCUSSION

The CNTs can be obtained by heating the material in the presence of a suitable amount of oxygen and catalyst. The fibrous material from natural sources have a large number of vascular bundles and contains cellulose, hemicellulose, and lignin, and can be used efficiently as a precursor for CNT. During our initial studies, we compared the dried sugarcane pulp/ bagasse with fresh cubes; the cubes demonstrate far better results than sugarcane pulp. In bagasse, the vascular bundles were collapsed due to mechanical processing and removal of water content, whereas SC cubes were fully moist and retained the integrity of the vascular bundle, hence selected as a precursor for the fabrication of CNTs. A small amount of water and lignin plays an important role in the conversion of carbon black to CNTs

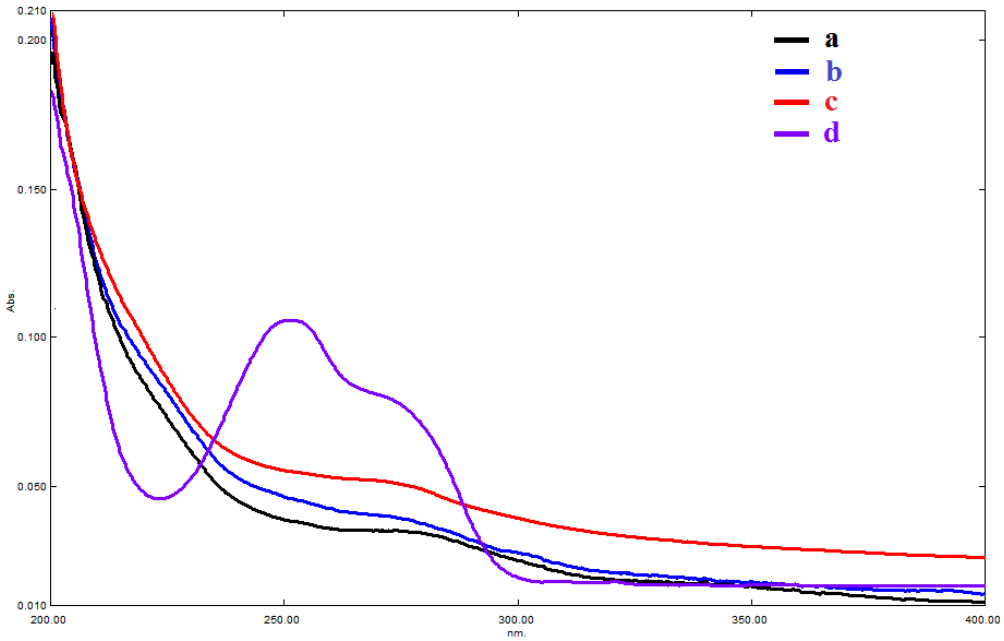

Fig. 1. UV-visible spectra of a) Standard CNT, b) Synthesized CNT, c)fCNT, d)ACV.

[18]. Purification of CNTs is necessary for designing material for biomedical as well as pharmaceutical applications. The researchers around the globe are focusing on green and eco-friendly routes for the synthesis of nanomaterials. These routes pave a way to enhance utility and applications in the multidisciplinary field of study. The eco-friendly methods enable the use and enhance the performance characteristics of CNTs in drug delivery and tissue engineering applications.

During synthesis method optimization, we used different sets of temperatures ranging from 200 – 500 ^{0}C with two-time points for the heating process i.e. 10 and 15 min as represented in table S1. The preliminary confirmation of synthesized CNTs was done using UV-vis spectrophotometric and FTIR analysis. For comparison purpose, we procured a standard commercial grade of MWCNTs (specifications: Multiwall CNT > 98% carbon basis, O.D. × I.D. × L 12 nm ± 1 nm × 5.5 nm ± 0.5 nm × 4-~7µm (Synthesis Method –Catalytic Chemical Vapour Deposition (CVD)). Less conversion rate was observed at the initial temperature of 200 ^{0}C, for 10 min as well as prominent peaks were missing in the UV-Vis and FTIR spectra. The reaction performed at 500 ^{0}C for 10 min, we found a distinct peak with less intensity as compared to standard CNT. After increasing the time for 15 min at 500 ^{0}C temperatures, a prominent peak was observed and matches with standard CNT, as represented in Fig. 1a. The closed-loop copper tube provides a favourable environment for catalytic conversion of carbon black to CNTs. It minimizes the oxygen interference during synthesis and prevents direct oxidation of the catalyst. The closed-loop environment also helps in increasing the catalytic performance of ferrocene.

UV-Vis Spectrophotometer (UV-Vis)

Preliminary evaluation of synthesized CNTs, fCNTs, and DLCNTs was performed using UV-Vis spectroscopy. The preliminary data gave an idea of the conversion rate during the synthesis process. Temperature, time of heating, and environmental oxygen were the three major constraints considered during the optimization of the synthesis process. The oxygen contact was minimized using a closed-loop copper tube and simultaneously temperature (500 ^{0}C) and time was optimized as represented in table S1. The UV-Vis spectra of standard CNTs show absorbance maxima at 260 nm, which may be due to π-π* transition of aromatic C-C bonds as represented in Fig. 1a. The absorbance maxima of standard CNTs were compared with synthesized CNTs. The processing temperature at 500 ^{0}C for 15 min provides

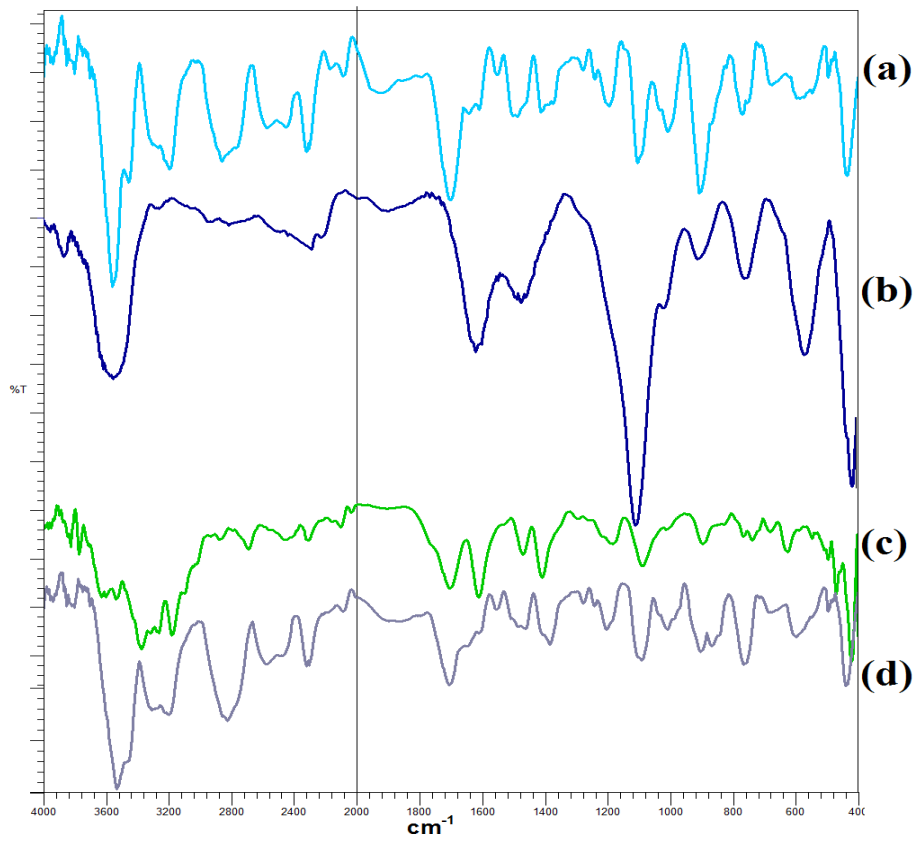

Fig. 2. FTIR spectrum of a) synthesized CNT, b) fCNT, c) DLCNT, d) Acyclovir.

distinctly similar peaks that of the standard CNTs (Fig. 1b). This spectrophotometric comparison preliminarily confirmed the conversion of carbon black to efficient, usable carbon nanotubes.

Fig. 1c, represents purified and functionalized CNTs (fCNTs), it shows slight increase in the peak intensity at an equivalent concentration as compared with Fig. 1a. The increase in peak intensity could be correlated with embedded hydroxyl and carboxyl functional groups on the surface, which was confirmed further using FTIR spectra. The absorption maxima for fCNTs was shifted to 258 nm, this may be due to the removal of amorphous carbon after the purification step. The purification helps to increase CNTs dispersibility in water and reduces noise in the spectrum. Previous studies proved a strong relationship between the absorption maxima and the diameter of CNTs. After purification, the CNTs may expand slightly, where p electron Plasmon helps to increase the absorption maxima, which can be correlated with an increase in diameter of CNTs and vice versa [19].

A prominent absorbance maxima at 251 nm was found in the UV-Vis spectra of ACV, which was in accordance with the reported literature (Fig. 1d) [20]. The absorbance maxima help to identify the purity of the drug as well as to estimate the concentration of ACV in DLCNT. The amount of ACV loaded in DLCNTs was estimated using the UV-Vis Spectra at 251 nm from supernatant obtained after centrifugation in DMSO. The *in-vitro* drug release characteristics were studied by recording absorbance at 251 nm in withdrawn samples at a predetermined time interval during the dissolution study.

Fourier Transform Infrared Spectroscopy (FTIR)

The FTIR Spectroscopy was performed to identify the functional groups from CNTs and fCNTs. Fig. 2a shows the typical IR spectra of the sample, which was obtained by the successive heating treatment at about 500 ˚C. The strong multiple peaks around 3600 cm^{-1} represent hydroxyl stretching vibration, while peaks around

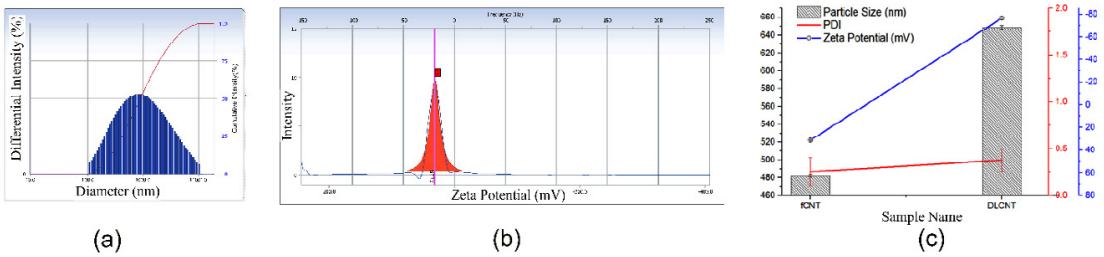

Fig. 3. Particle size (a) Zeta potential analysis (b) analysis of fCNTs. Comparative particle size, zeta potential and PDI of fCNTs and DLCNTs (c).

2800 cm^{-1} represent C-H stretching mode. The peak at 1618 cm^{-1} is associated with the vibration of the carbon skeleton of the CNT. The peaks at about 1712 and 1550 cm^{-1} indicate the existence of the C=O and C=C groups and emerged due to the presence of functional groups like carboxylic acid, ketone, quinone, epoxy, etc. The multiple bands were observed in the range of 1302–900 cm^{-1}, which might be due to the presence of C-O stretching and bending mode [21].

After the purification process of CNTs, the sharp peaks were emerged and new distinct vibrational intensities were reflected in fCNT (Fig. 2b) with a decrease in noise. A strong intense broad peak was observed around 3500–3400 cm^{-1} due to hydroxyl stretching vibration and associated moisture. Two small peaks were appeared at 3150 cm^{-1}, which confirms the embedded surface hydroxyl group on fCNTs. Fig. 2(b) shows a strong absorption band at 1712 cm^{-1} which is attributed to the carboxylic group (C=O), and a band at 1580 cm^{-1} corresponds to C=C. The strong distinct peak around 1150 cm^{-1} was observed due to C-O stretching vibrations. A similar intense peak at 1058 cm^{-1} was observed due to the epoxy or alkoxy group (C-O) [21]. These peaks indicate the presence of oxygen-containing groups on fCNTs. As depicted in Fig. 2b, the conversion of natural SC bagasse into the carbon skeleton in the form of carbon nanotubes was confirmed. The spectrum showed noise before purification, which was disappeared during a purification step with nitric acid and ammonia solution [22].

The carbodiimide chemistry approach helps to graft ACV on carboxyl functional fCNTs. The intensity of the carboxyl groups decreases with the emergence of new bonds like an amide as represented in Fig. 2c. The peak intensity decreases at a peak around 3600 cm^{-1} with the emergence of a new sharp peak around 3474 cm^{-1}, attributed to N-H stretching vibrations. The emergence of a peak around 3198 represents secondary amine from ACV. The two broad peaks at 1758 and 1672 cm^{-1} were emerged due to the presence of C=O and –CONH amide I stretching, respectively [10]. The small peak around 1563 cm^{-1} was appeared due to CONH amide II stretching vibration and indicates the successful decoration of ACV on the surfaces of fCNT via amide bonding between a carboxylic group of fCNT and the amine group of ACV [23]. The peak attributed at 1401 cm^{-1} shows bending of carboxylic –OH group, which suggests that after ACV grafting, the carboxylic groups remain available for therapeutic activity. The peak around 1265 cm^{-1} was assigned for C-N stretching vibrations.

The FTIR spectrum of ACV was in accordance with the reported in the literature [24] and was exhibiting characteristic peaks of primary and secondary amines near 3297 cm^{-1}. As shown in Fig. 2d, a peak near to 3458 cm^{-1} was observed for the hydroxyl group. A peak at 1650 cm^{-1} was due to the C=C and a peak at 1715 cm^{-1} was appeared due to the C=O carboxyl group of ACV [25, 26]. The presence of ACV in DLCNTs was confirmed from the spectra as depicted in Fig. 2c and was compared with pure ACV intensities, which demonstrates successful grafting after carbodiimide chemistry.

Particle size and Zeta potential analysis

The particle size is the fundamental factor for multidimensional carbon allotropes. Dynamic light scattering (DLS) is not the perfect method to access the particle size of CNT due to the L/D ratio. The preliminary changes in the hydrodynamic diameter of samples were identified using the DLS method. The average particle size of fCNTs was found to be 482±1.5 nm (Fig. 3a), while in the case of DLCNTs, it was slightly increased and found around 649.5±1.89 nm (Fig. 3c). This type

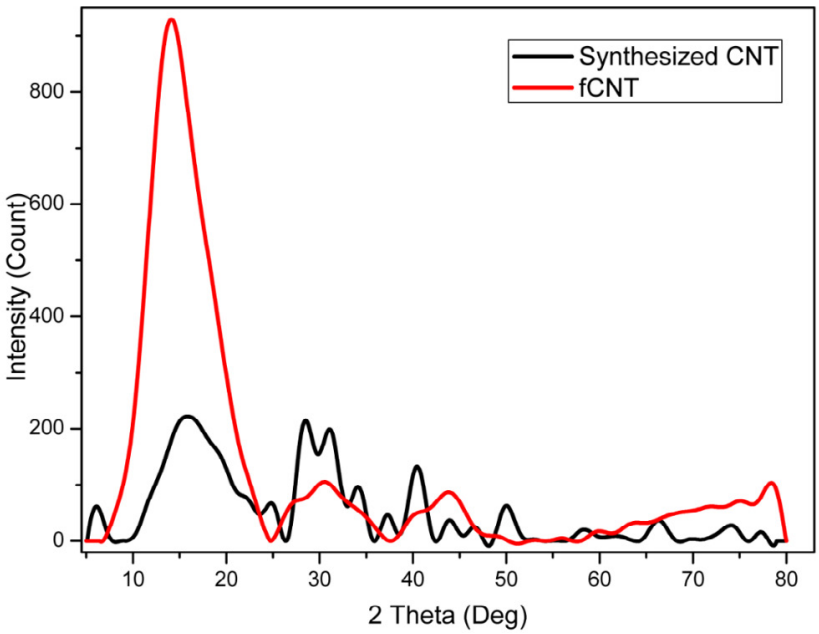

Fig. 4. XRD analysis of synthesized CNT and fCNT.

of size enlargement might be due to one of the dimensional array from the nanotube section which was larger in length as well as due to the deposition of drug crystals.

The CNTs do not provide correlative particle size using DLS, as one of the dimensions from the tube is larger and the aspect ratio is high (>10^3) as well as shapes are far from spherical [27]. The zeta potential analysis of fCNT and DLCNT suspensions is shown in Fig. 3b and c. Zeta potential signifies that stability of dispersion is being for a longer period, as dispersed CNTs were not settled for more than 48 h.

X-ray diffraction (XRD) analysis

The XRD pattern of CNTs produced from partially oxidized SCB precursor after the high-end heat treatment is depicted in Fig. 4. The mechanism involves the conversion of amorphous carbon black to crystalline nanotubes, due to the catalytic behaviour of ferrocene at optimum temperature. It also suggests that some other crystalline carbon impurities were removed during the purification step.

The XRD pattern from synthesized CNTs reveals various peaks at 2 Theta position of 24.8, 28.5, 31.1, 34.1, 40.4 and 50 degrees with corresponding Millar indices (1 1 1), (2 0 0), (2 0 0), (2 1 0), (2 2 0), (2 2 2) respectively. It suggests that 27.03, 30.57, 43.59 degrees correspond to (1 0 0), (1 0 0), (1 1 1) planes of carbon in a hexagonal structure.

The calculated average crystallite size (Scherer equation) of synthesized CNTs was found to be 42.84 and 44.45 nm respectively; it was also in accordance with the morphological observation as confirmed simultaneously using SEM analysis.

Raman spectroscopy

The stretching of the hexagonal ring structure from the crystallite of graphitic carbon materials has emerged with a small peak as D band. An emergence of D band simultaneously with the G band reflects the vibrations associated with the breathing mode of sp^2 hybridized carbon rings. The intensity difference between the G and D bands represents the purity of CNTs. If the intensity is lesser for D band, it represents the highest purity in fCNTs and could be confirmed by elemental analysis. The D and G band, intensities correlate the interlayer spacing or diameter in the fCNTs, the value I_D/I_G was found to be 0.8742, corresponds to the reasonable crystalline quality of CNTs after heat treatment [28-31].

In the Raman spectra of synthesized CNTs and fCNTs, the D band was observed at around 1361 cm^{-1} and 1390 cm^{-1} respectively (Fig. 5). In synthesized CNTs, the broadband was appeared due to the presence of amorphous carbon that

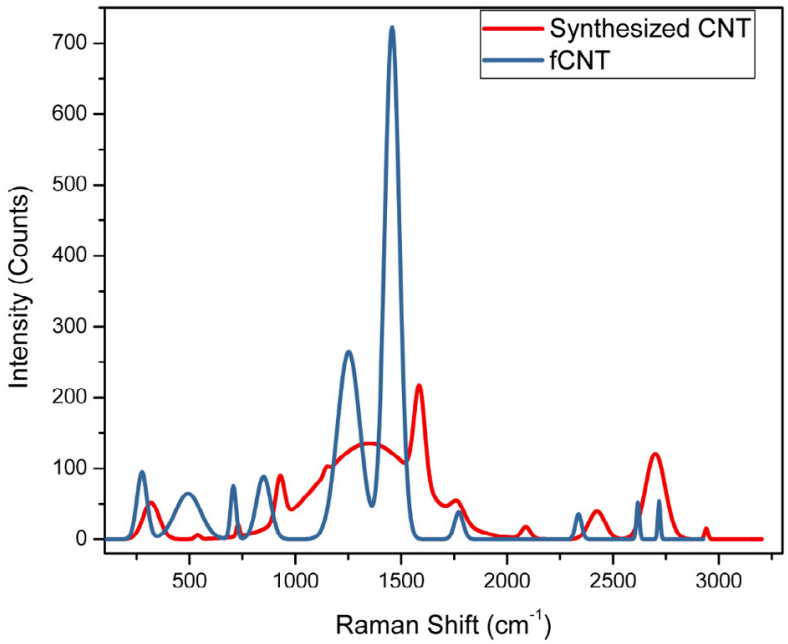

Fig. 5. Raman spectra of synthesized CNT and fCNTs.

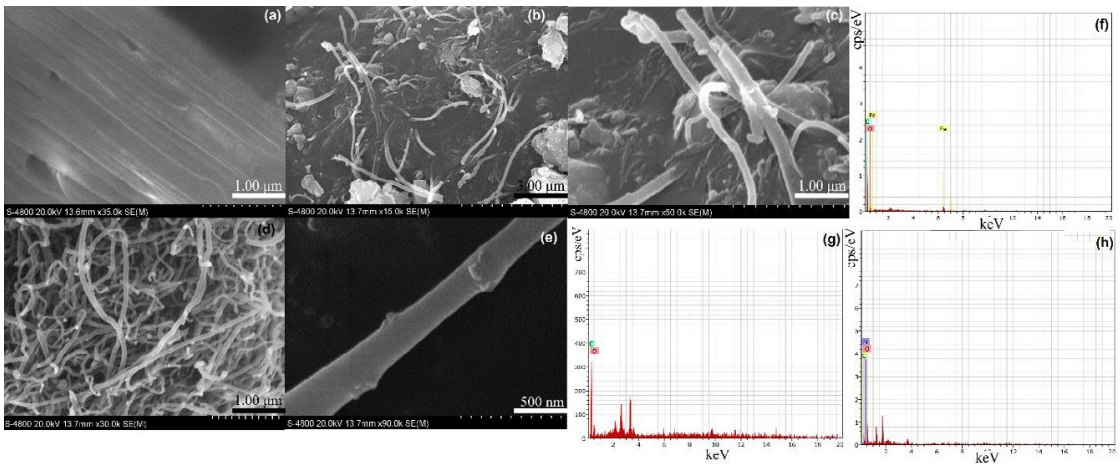

Fig. 6. SEM images of a) CNT at temp. 500 °C without catalyst, b & c) Synthesized CNT with catalyst, d) Purified fCNT, e) fCNT at 500 nm, EDX spectra of, f) Synthesized CNT, g) fCNT, h) DLCNT.

protects the vibrational frequency of CNTs. The corresponding G band has emerged at 1594 and 1590 cm^{-1} in synthesized CNT and fCNTs with a less intensity, but was increased at a sharp edge after the purification process. The Two phonons spectra (2D band) observed around 2693 and 2841 cm^{-1} was due to phonon defect interaction in sp^2 hybridized carbon [28-31]. Other peaks observed between 100–600 cm^{-1} were due to radial breathing mode, correlates to the highest purity, and the thin innermost layer with low defects [32].

Scanning Electron Microscopy (SEM) and Elemental Analysis (EDX)

In the CNT synthesis process, at the lowest temperature rate without a closed-loop copper tube, a very less conversion rate was observed compared to the optimum temperature and closed-loop copper tube. Fig. 6a shows carbonaceous material obtained from SCB with fibrous undivided materials. Soon after modification of the reaction using ferrocene catalyst, the fragmented portions of separated nanotubes along with amorphous

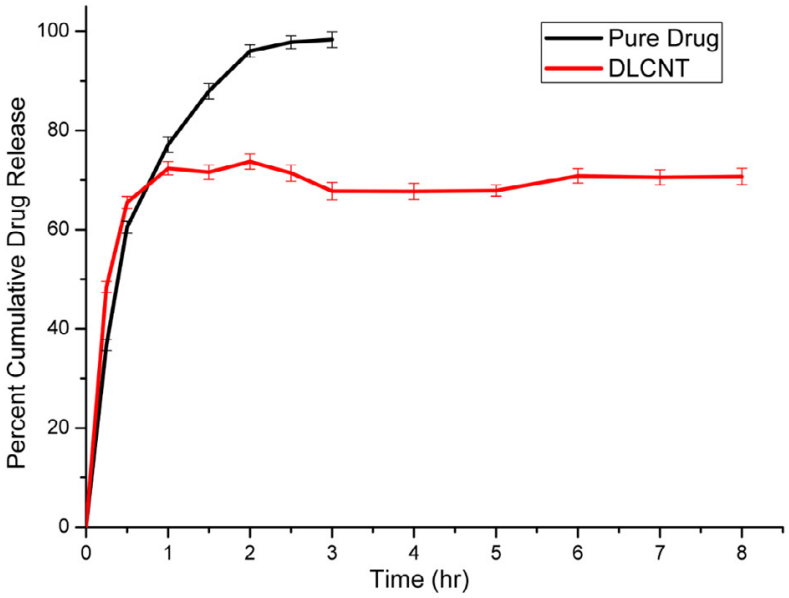

Fig. 7. *In-vitro* drug release of pure drug and drug loaded CNT.

carbon were observed as depicted in Fig. 6b and 6c. The purified CNT (fCNT) bunch was observed after reaction under controlled conditions in an acidic medium. Due to the presence of nitric acid, ammonia solution the amorphous carbon along with other catalytic impurities gets dissolved, hence the separated nanotubes can be observed in Fig. 6 d and e. At lower resolution up to 500 nm, a single fragment of CNTs represents successful conversion of natural precursor to CNTs by preserving its backbone (Fig. 6e). The fCNT indicates the comprehensible morphologies with long tubular structures at nanoscale dimensions. The wide range of size was found in between 30 -90 nm, it was also reflected from XRD analysis by Scherrer equation. A closed-loop of supercoiled structure in SEM images signifies the CNT was formed in the presence of a catalyst at specific temperature conditions. The tubular structure is basically due to the vascular bundles of SCB and retains rigidity at higher temperature cycles with an oxidative environment due to the presence of a catalyst [33].

Elemental mapping of synthesized CNTs and fCNT was performed for elemental content (Fig. 6 f, g, and h). The solid net atomic percentage was compared, which could help to calculate the exact percentage of elements available after sample analysis. The EDX spectra of synthesized CNT were represented in Fig. 6f shows presence of atomic percentage of elements as 76.85% of carbon, 18.73% of oxygen, and 4.42% of Fe confirms the carbonaceous structure formation. The purification step improved the quality of CNT by removing amorphous carbon, and metal ion impurities. The peak of Fe was disappeared after purification in the presence of a strongly acidic environment. The carbon and oxygen concentration (68.39%, 31.61% respectively) was changed; the concentration of oxygen was significantly enhanced due to the enrichment of oxygen functional group grafted on the surfaces. The decrease in carbon percentage implies that some of the amorphous carbon was removed after following the purification steps. As shown in supplementary data of percentage drug content, the model drug was successfully embedded within DLCNTs and can summarily be confirmed by the presence of nitrogen element in the EDX spectra of DLCNT. The percentage of carbon (31.52%), oxygen (65.28%), and nitrogen (3.20%), signifies that the ACV was successfully loaded on DLCNTs.

In-vitro Drug Release

The ACV was used as a model drug and loaded on DLCNTs using an active loading approach. The *In-vitro* drug release study was performed in pH 7.4 phosphate buffer and the percentage

cumulative drug release pattern is depicted in Fig. 7. During *In-vitro* drug release study, samples were withdrawn at predetermined interval of time and absorbance was recorded (Fig. 1d). The pure ACV demonstrated complete release within 3 h corresponds to immediate-release, while DLCNTs retarded the drug release up to 8 h. At the initial 2 h of the study, the ACV released rate from DLCNTs was rapid and may be due to passive loaded ACV available within the internal structure of DLCNTs. At the later stages, the ACV release rate was retarded up to 8 h. The DLCNT follows a slow and sustained release effect [34, 35]. The formation of amide bonding between two different substrates using a crosslinking mechanism can also be used for other amine and carboxyl functional drugs. Most of the proteins or peptides molecules have carboxylic or amine functionality, hence they can possibly load over the allotropic forms of carbon-containing carboxylic functionality. Such modulation can provide effective delivery to the targeted site and retard the release rate.

CONCLUSION

The present investigation was aimed to develop a facile method for the synthesis of CNTs using SCB as a precursor material along with its fabrication and purification for biomedical applications. This economically feasible as well as eco-friendly process avoids the emission of toxic gases during the synthesis of CNTs. The UV Spectroscopic studies helped to confirm the presence of π- π* transition of aromatic C-C bonds preliminarily at 260 nm. The FTIR spectra were used to elucidate the major functional groups present in synthesized CNTs and fCNTs, and verified using reported literature. The ACV was used as a model drug for loading over fCNTs. The ACV loading was confirmed by using UV-visible spectroscopic analysis, FTIR, and elemental analysis. The structural morphology of synthesized CNTs was observed using SEM images, it showed the cluster of hollow cylindrical tubes and was differentiated from fCNT. The amorphous carbon from synthesized CNTs was removed utilizing purification steps and the samples were analysed using XRD, Raman, and SEM data. The SCB is a renewable natural precursor, which could be used for the synthesis of CNTs. Any fibrous material from natural origin may contain a small amount of water that can help in the oxidation process during the fabrication of CNTs. It will also help in oxidizing the organic material at higher temperature conditions and provides an effective environment for catalysis. The closed-loop copper tube avoids direct contact with external oxygen and maintains the inner environment for catalytic conversion. Elemental modalities represent the presence of traces of impurities in synthesized CNTs, whereas purified fCNTs were free from iron impurities. The percentage cumulative drug release from fCNTs demonstrated sustained effect up to 8h. The fCNTs can be an effective candidate for tissue engineering and drug delivery applications. These types of approaches could be helpful for designing an active targeted drug delivery system by loading ligands on the CNTs. The surface grafting potential of CNTs is very high as compared to other nanomaterials, moreover passive and active loading could also be performed. The protein and peptide-based drugs might be a suitable candidate to deliver effectively at a targeted site.

ACKNOWLEDGMENT

Authors are thankful to Dr. Sanjay Bachchav RCPACS, Shirpur, India for providing Standard CNT sample. Authors are also thankful to the Management, Principal for providing Research Facilities for progression of work.

CONFLICT OF INTEREST

The authors declare that they have no conflict of interest.

REFERENCES

[1] Iijima S., (1991), Helical microtubules of graphitic carbon. *Nature.* 354: 356-364.

[2] Hirlekar R., Yamagar M., Garse H., Vij M., Kadam V., (2009), Carbon nanotubes and its applications: A review. *Asian J. Pharmac. Clinical Res.* 2: 17-27.

[3] Fathy N. A., Basta A. H., Lotfy V. F., (2020), Novel trends for synthesis of carbon nanostructures from agricultural wastes. *Carbon Nanomater. Agri-Food Environm. Appl. (Micro and Nano Technol.).* 59-74.

[4] Szabó A., Perri C., Csató A., Giordano G., Vuono D., Nagy J. B., (2010), Synthesis methods of carbon nanotubes and related materials. *Materials.* 3: 3092-3140.

[5] Fathy N. A. (2017), Carbon nanotubes synthesis using carbonization of pretreated rice straw through chemical vapor deposition of camphor. *RSC. Adv.* 7: 28535-28541.

[6] Janas D., (2020), From bio to nano: A review of sustainable methods of synthesis of carbon nanotubes. *Sustainability.* 12: 4115-41131.

[7] Vivekanandhan S., Schreiber M., Muthuramkumar S., Misra M., Mohanty A. K., (2017), Carbon nanotubes from renewable feedstocks: A move toward sustainable nanofabrication. *J. Appl. Polym. Sci.* 134: 44255-44262.

[8] Suriani A., Dalila A., Mohamed A., Mamat M., Salina M., Rosmi M., Rosly K., Roslan M. N., Rusop M., (2013),

Vertically aligned carbon nanotubes synthesized from waste chicken fat. *Mater. Lett.* 101: 61-64.

[9] Garmaroudi F., Vahdati R., (2010), Functionalized CNTs for delivery of therapeutics. *Int. J. Nano Dimens.* 1: 89-102.

[10] More M., Ganguly P., Pandey A., Dandekar P., Jain R., Patil P., Deshmukh P. K., (2017), Development of surface engineered mesoporous alumina nanoparticles: Drug release aspects and cytotoxicity assessment. *IET Nanobiotechnol.* 11: 661-668.

[11] More M. P., Deshmukh P. K., (2020), Development of amine-functionalized superparamagnetic iron oxide nanoparticles anchored graphene nanosheets as a possible theranostic agent in cancer metastasis. *Drug. Deliv. Transl. Re.* 2020: 1-16.

[12] More M. P., Chitalkar R. V., Bhadane M. S., Dhole S. D., Patil A. G., Patil P. O., Deshmukh P. K., (2019), Development of graphene-drug nanoparticle based supramolecular self assembled pH sensitive hydrogel as potential carrier for targeting MDR tuberculosis. *Mater. Technol.* 34: 324-335.

[13] Shirazi Y., Tofighy M. A., Mohammadi T., Pak A., (2011), Effects of different carbon precursors on synthesis of multiwall carbon nanotubes: Purification and functionalization. *Appl. Surf. Sci.* 257: 7359-7367.

[14] Naderi A., Abdi Tahne B., (2017), Band bending engineering in pin gate all around Carbon nanotube field effect transistors by multi-segment gate. *Int. J. Nano Dimens.* 8: 341-350.

[15] Qureshi D., Nadikoppula A., Mohanty B., Anis A., Cerqueira M., Varshney M., Pal K., (2021), Effect of carboxylated carbon nanotubes on physicochemical and drug release properties of oleogels. *Colloid. Surf. A.* 610: 125695-125701.

[16] He H., Pham-Huy L. A., Dramou P., Xiao D., Zuo P., Pham-Huy C., (2013), Carbon nanotubes: Applications in pharmacy and medicine. *Biomed. Res. Int.* 2013: 12-19.

[17] Heidarian M., Khazaei A., Saien J., (2021), Grafting drugs to functionalized single-wall carbon nanotubes as a potential method for drug delivery. *Phys. Chem. Res.* 9: 57-68.

[18] Kang Z., Wang E., Mao B., Su Z., Chen L., Xu L., (2005), Obtaining carbon nanotubes from grass. *Nanotechnol.* 16: 1192-1197.

[19] Rance G. A., Marsh D. H., Nicholas R. J., Khlobystov A. N., (2010), UV–vis absorption spectroscopy of carbon nanotubes: Relationship between the π-electron plasmon and nanotube diameter. *Chem. Phys. Lett.* 493: 19-23.

[20] Tavares G. D., Ishikawa G. M., Monteiro T. F., Zanolini C., Kedor-Hackmann É. R. M., Bou-Chacra N. A., Consiglieri V. O., (2012), Derivative spectrophotometric method for determination of acyclovir in polymeric nanoparticles. *Quím. Nova.* 35: 203-206..

[21] Stobinski L., Lesiak B., Kövér L., Tóth J., Biniak S., Trykowski G., Judek J., (2010), Multiwall carbon nanotubes purification and oxidation by nitric acid studied by the FTIR and electron spectroscopy methods. *J. Alloy. Compd.* 501: 77-84.

[22] Patterson A., (1939), The scherrer formula for X-ray particle size determination. *Phys. Rev.* 56: 978-983.

[23] Yang M.-H., Jong S.-B., Lu C.-Y., Lin Y.-F., Chiang P.-W., Tyan Y.-C., Chung T.-W., (2012), Assessing the responses of cellular proteins induced by hyaluronic acid-modified surfaces utilizing a mass spectrometry-based profiling system: Over-expression of CD36, CD44, CDK9, and PP2A. *Analyst.* 137: 4921-4933.

[24] Shoukat H., Pervaiz F., Noreen S., Nawaz M., Qaiser R., Anwar M., (2020), Fabrication and evaluation studies of novel polyvinylpyrrolidone and 2-acrylamido-2-methylpropane sulphonic acid-based crosslinked matrices for controlled release of acyclovir. *Polym. Bull.* 77: 1869-1891.

[25] Karolewicz B., Nartowski K., Pluta J., Górniak A., (2016), Physicochemical characterization and dissolution studies of acyclovir solid dispersions with Pluronic F127 prepared by the kneading method. *Acta Pharmaceut.* 66: 119-128.

[26] Mahmood A., Ahmad M., Sarfraz R. M., Minhas M. U., Yaqoob A., (2016), Formulation and *in vitro* evaluation of acyclovir loaded polymeric microparticles: A solubility enhancement study. *Acta Pol. Pharm.* 73: 1311-1324.

[27] Li Z., Luo G., Zhou W., Wei F., Xiang R., Liu Y., (2006), The quantitative characterization of the concentration and dispersion of multi-walled carbon nanotubes in suspension by spectrophotometry. *Nanotechnol.* 17: 3692-3696.

[28] Yano T., Ichimura T., Kuwahara S., H'Dhili F., Uetsuki K., Okuno Y., Verma P., Kwata S., (2013), Tip-enhanced nano-raman analytical imaging of locally induced strain distribution in carbon nanotubes. *Nat. Commun.* 4: 2592-2596.

[29] Cuesta A., Dhamelincourt P., Laureyns J., Martinez-Alonso A., Tascón J. D., (1994), Raman microprobe studies on carbon materials. *Carbon.* 32: 1523-1532.

[30] Heise H., Kuckuk R., Ojha A., Srivastava A., Srivastava V., Asthana B., (2009), Characterisation of carbonaceous materials using Raman spectroscopy: A comparison of carbon nanotube filters, single and multi walled nanotubes, graphitised porous carbon and graphite. *J. Raman Spectrosc.* 40: 344-353.

[31] Asokan V., Myrseth V., Kosinski P., (2015), Effect of Pt and Fe catalysts in the transformation of carbon black into carbon nanotubes. *J. Phys. Chem. Solids.* 81: 106-115.

[32] Zhao X., Ando Y., Qin L.-C., Kataura H., Maniwa Y., Saito R., (2002), Radial breathing modes of multiwalled carbon nanotubes. *Chem. Phys. Lett.* 361: 169-174.

[33] Allaedini G., Tasirin S. M., Aminayi P., Yaakob Z., Meor Talib M. Z., (2016), Carbon nanotubes via different catalysts and the important factors that affect their production: A review on catalyst preferences. *Int. J Nano Dimens.* 7: 186-200.

[34] Farahani B. V., Behbahani G. R., Javadi N., (2016), Functionalized multi walled carbon nanotubes as a carrier for doxorubicin: Drug adsorption study and statistical optimization of drug loading by factorial design methodology. *J. Brazil. Chem. Soc.* 27: 694-705.

[35] Ghoshal S., Kushwaha S. K. S., Srivastava M., Tiwari P., (2014), Drug loading and release from functionalized multiwalled carbon nanotubes loaded with 6-mercaptopurine using incipient wetness impregnation method. *Am. J. Adv. Drug Deliv.* 2: 213-223.